

EXECUTIVE SUMMARY

Seismic Testing

Geogrid Reinforced Soil Structures
Faced with Segmental
Retaining Wall Block



by Columbia University

In cooperation with
Allan Block Corporation
Huesker Geosynthetics

Seismic Testing For Allan Block and Huesker Synthetic

Table of Contents

Columbia University	Pg. 1
Introduction	Pg. 2
Executive Summary	Pg. 3
Testing Summary/Results	Pg. 7
Testing Photos	Pg. 9
Design Methodology	Pg. 11
External Stability	Pg. 14
Internal Stability	Pg. 19
Summary of Calculations	Pg. 23
Allan Block & Huesker Synthetics	Pg. 25

Columbia University

Columbia University was founded in 1754 as King's College by royal charter of King George II of England. It is the oldest institution of higher learning in the state of New York and the fifth oldest in the United States.

Since the first class in July of 1754 until today, the college has emerged as a preeminent national center for educational innovation and scholarly achievement.

Thanks to concerted efforts to place the University on the strongest possible foundations, Columbia is approaching the twenty-first century with a firm sense of the importance of what has been accomplished in the past and confidence in what it can achieve in the years to come.



Full Scale Seismic Testing:

Setting new standards for SRW design and performance

Teamwork often produces events that individuals are not capable of on their own. So was the case when Columbia University, Allan Block Corporation and Huesker Inc. teamed up to conduct full scale seismic testing on a group of geogrid reinforced soil structures faced with a segmental retaining wall block. The first-ever-full scale testing took place in Tsukuba, Japan in cooperation with Dr. Yoshiyuki Mohri at the National Research Institute of Agriculture Engineering. Professor Hoe Ling from Columbia University and Professor Dov Leshchinsky from the University of Delaware, headed up the team as the Principle Investigators of the ground breaking research.

Most research to this point had focused on the individual components of the structure and performance in static conditions. Much of the research had indicated an overly conservative approach was used by over estimating loads and underestimating the system performance of the geogrid reinforced SRW structures. Yet as is customary in the engineering world, change is not easily achieved. The intent of this study was to not only evaluate and substantiate system performance with dynamic excitations, but illustrates the basic performance characteristics of these systems when used in static environments.

The basic reinforcement configuration used on the test structures simulated typical designs found in structures for static loading conditions. Therefore it was expected that the first of the three test structure would experience some type of catastrophic failure. In fact the first structure performed so well under the initial excitations that the magnitude of the load was doubled and still performed extremely well.

An underlying question that has slowed the growth of these systems in many highway applications has been the issue of a positive mechanical connection between the geogrid and the SRW block facing. Many in the engineering community have theorized that without a mechanical connection the system was subject to premature failure in static and seismic loading conditions. It was therefore the intent of this study to validate the performance of a system that created a "rock-lock" frictional connection between the SRW facing and the layers of geogrid reinforcement. Additionally, if an earthquake event that exceeded the magnitude of the Kobe earthquake from 1995 (7.2 on the Richter scale) could not damage these composite structures, we could in fact validate performance for these structures in all environments.

This document contains an executive summary of this first round of seismic testing on SRW structures and one set of hand calculations that were performed to predict the performance of the structures. For more information contact the Allan Block Corporation.

Research Team:

Professor Hoe Ling, Department of Civil Engineering, Columbia University
Professor Dov Leshchinsky, Department of Civil Engineering, University of Delaware

Chief Collaborators

Dr. Yoshiyuki Mohri, National Research Institute of Architectural Engineering, Japan Ministry of Agriculture, Forestry and Fisheries
Mr. Kenichi Matsushima, National Research Institute of Architectural Engineering
Dr. Mutsuo Takeuchi, National Research Institute of Architectural Engineering, Structural Division

Authors:

Professor Hoe Ling
Professor Dov Leshchinsky
Tim Bott, Allan Block Corporation

Executive Summary for Seismic Testing performed by Professor Hoe Ling, Columbia University and Professor Dov Leshchinsky, University of Delaware in 2002

Overview:

Reinforced soil structures faced with segmental retaining walls have become a cost effective solution for retaining walls in residential, commercial and governmental land development. Over the past fifteen years the use of these types of systems has spurred a historical evolution in retaining wall design and construction. Change is seldom readily embraced within the Civil Engineering community, but the merits of geogrid reinforced soil structures captured the attention of the design and building community. Use of segmental blocks in conjunction with geogrid-reinforced soil has become a significant percentage of the different types of retaining walls. To date, most research has been compiled through numerical modeling, from instrumentation of walls and reduced scale laboratory tests in static loading conditions. The intent of this venture is to evaluate the true performance characteristics under realistic earthquake loading to substantiate these systems for both seismic and static conditions.

Objectives:

- To analyze the internal and external performance characteristics of a full-scale geogrid reinforced soil mass with a concrete segmental wall facing when significant earthquake loads are applied to the structure.
- To determine the ramification of earthquake loading on current design standards and modify the design and reinforcement parameters to ensure a safe and cost effective design solution.
- To evaluate observed behavior and loads when compared to design calculations.
- To evaluate the effectiveness of a block to geogrid connection based on rock-lock achieved through a hollow core concrete unit.
- To determine the performance characteristics of a structure with Fortrac geogrids in combination with Allan Block retaining wall units.
- To avoid possible scaling problems associated with reduced scale model tests, full-scale walls were constructed using prototype blocks and geogrids.

Facilities and test setup:

Materials:

A fine uniform sand with an angle of internal friction of 38° and an optimum dry density of 15 kN/m^3 was used as the reinforced, retained and foundation soil.

Geogrids: Two types of Fortrac geogrids, manufactured by Huesker, were used in the study. Fortrac 35/20-20 (PET, polyester) was used in all three tests, and in Test 3, the top layer of reinforcement was Fortrac 20 MP (PVA, polyvinyl alcohol) to illustrate the ability of the system to incorporate a rigid connection by grout-filling the top two courses of block. PVA geogrid was utilized due to its strong resistance against an alkaline environment. As the names indicate the strength of these grids are 35 kN/m and 20 kN/m respectively.

Concrete segmental wall facing: Allan Block retaining wall blocks were used in all three tests. The units were 200 mm high by 300 mm deep by 450 mm wide. The unique element of the Allan Block wall product is hollow cored units with a raised front shear key and the corresponding notch on the bottom front surface. The configuration of the block assemblies used for testing provided a 12° setback of the facing. The hollow core unit weighs 34 kg and provides a configuration, which locks the geogrid into the wall assembly when the cores of the block are filled with compacted gravel.

Input Motion:

The motion in the Kobe earthquake was used since it represented a significant case history, magnitude of 7.2, which was well recorded and documented. Therefore the planned excitation would develop accelerations that met or exceeded the recorded results of the Kobe earthquake on January 17, 1995. The peak accelerations for different components of Kobe earthquake are compiled in Table 1:

Table 1: Peak Accelerations for Different Components of Kobe Earthquake

Directions	Peak Accelerations
NS	0.59g
EW	0.63g
UD	0.34g

Two horizontal excitations were applied for each of the three tests. In the first excitation, the peak was scaled to 400 gal (0.4 g) and in the second, it was scaled to 800 gal (0.8 g). The second shaking was applied an hour after the application of the first excitation was completed. There were no modifications to the structure between the first and second shaking. Vertical excitations were applied to the third test, with the peak acceleration first scaled at 200 gal (0.2 g) and the second scaled at 400 gal (0.4 g), i.e., half the value of the peak horizontal accelerations.

Construction:

A three-sided steel box (2 m wide by 4 m deep by 3 m high) was built to provide a framework for the test on top of the shake table. To prevent reflection waves from the steel wall surfaces during shaking, EPS boards were placed at the front and back ends of the steel box. Side friction between the backfill and box was reduced using a layer of grease, which was isolated from the sand with sheets of plastic.

Sand was placed in 200 mm lifts and compacted with a hand operated plate compactor. Water was mixed with the sand to achieve the desired density and compaction. Compaction results of 94% of standard proctor were achieved during construction. Sand was placed directly to the back of the block with gravel only being placed into the cores of the block. The hand operated plate compactor was also used to densify the gravel in the cores of the block by running the compactor over the top of the blocks. Thin seams of white sand were placed at different heights to enable location of deformation and shear zones in the soil after completion of the test. Typical construction time for each structure was five to seven days.

Reinforcement Layout and Instrumentation:

Each wall was constructed to a height of 2.8 m with a 20 cm foundation layer of the same sand as the backfill. Detailed hand calculations were performed in advance of the testing using the Allan Block design methodology. Potential failure modes using these calculations indicated geogrid pullout from the soil at the top elevation was expected. An allowable displacement of 51 mm was used in the analysis.

Reinforcement lengths for Tests 1 and 2 was $L = 2.05$ m throughout the height of the wall. This equates to $0.73H$, where H is the wall height and is equal to 2.8 m. L was measured from the front end of the block. In Test 3, the length was reduced to 1.68 m ($0.6H$) for all but the top layer, which was 2.52 m ($0.9H$). The first layer of geogrid in each test was located on top of the first course of block. Vertical spacing after the first layer of geogrid was 60 cm, or every third course on Test 1 and 40 cm, every other course of block on Tests 2 and 3. The modification of reinforcement length and spacing was based on experience gained on each test and correlation of performance with calculated values.

A 100 channel data acquisition was used to record the instrumentation data during Tests 1 and 2. Multiple data acquisition systems were used on Test 3 as the total number of channels exceeded 100.

A total of 20 accelerometers were installed to measure the horizontal acceleration at various locations throughout the structure. Since vertical accelerations were introduced into Test 3, an additional set of 20 accelerometers was used to measure vertical acceleration. The vertical and horizontal excitations produced by the shaking table were also recorded.

Additional measurements were made to record the displacement at the face of the wall, settlement of the backfill and top of the block, lateral displacement of the backfill during shaking, earth pressure at the back of the block, vertical stress at the bottom of the block and base of the backfill, additional transducers at the bottom of the block to capture load potential load eccentricity, and heavily instrumented geogrid layers to evaluate magnitude and location of stress in each layer of geogrid. During construction, the data was logged at an interval of one to two minutes, but for dynamic tests, the data-logging interval was 0.002 seconds.

Visual Observations:

Each wall structure showed, at most, hairline cracks at the rear end of the reinforcement after the first shaking. These observations coincided with expected results from initial hand calculations. At the completion of the second set of shaking, shallow cracks were observed at the surface, mainly behind the reinforcement. Settlement was observed only after the second excitation. The settlement was significantly reduced with the change in geogrid spacing from 60 cm to 40 cm during Tests 2 and 3. The lenses of white sand did not reveal a distinct failure surface in the backfill. This supports the coherent mass concept of the design method used.

Wall Face Displacement:

Tests 1,2 and 3 each exhibited small wall face displacement during or at the conclusion of the 0.4 g excitation. Horizontal displacements of less than 10 mm were observed in each case. During and at the conclusion of the 0.8 g excitation horizontal displacements at the top of the first wall increased to approximately 80 mm. These results were also predictable based on pullout from the soil calculations of the top layer of geogrid and the allowable deformation of 51 mm used in the calculations. The increased geogrid length for Test 3 for the top layer of grid minimized the cracking and pushed the location of the crack further away from the block facing.

Lateral Earth Pressure:

There was minimal difference in results for the lateral pressure at the end of construction and before shaking. The pressure distribution was not consistent for all three walls. It is likely the pressure distribution was affected by the compaction during construction. However the earth pressure increased with shaking and trended with the displacement. The magnitude of the lateral earth pressure was less than the predicted load at the back of the block. This coincides with the load measured on the grid thus contradicting the notion that in all segmental block walls a substantial part of the calculated load in each layer of the grid is transferred to the facial connection.

Vertical Earth Pressure:

Pressure at the base was uniform along the length of the geogrid but an increase in load was seen, as measurements were taken closer to the wall. Test 3 recorded larger vertical pressures due to the greater vertical shaking load applied. This also questions the concept of hinge-height and the reduction of normal loads acting at the connection when battered wall systems are used in construction.

Backfill Surface Settlement:

Settlement after the first shaking (0.4 g) on all three structures was negligibly small. After the second shaking (0.8 g), the settlement was largest behind the reinforced soil zone where surface cracks developed. Test 1 exhibited the largest settlement behind the wall, which corresponds to the lowest pullout resistance in the soil of the top layer of grid and increased spacing between grid layers. Settlement in Test 2 was reduced from 80 mm after Test 1 to less than 20 mm with the geogrid spacing reduced from 600 mm to 400 mm. The settlement was reduced to approximately 10 mm in Test 3 with a reduction in basic grid length from 0.73H to 0.6H but increase in the top layer of grid to 0.9H. The top layer of geogrid was attached to the block facing with a standard flow-able grout to illustrate the ability of the system to incorporate a rigid connection at the top of the wall. Calculations for Test 3 indicate an increase of rear-end pullout resistance due to longer embedment length of the geogrid in a soil zone where overburden pressure is low. This supports the reduction in displacement at the face and corresponding reduction in settlement.

Tensile Load in Geogrid:

The results showed that the largest strain developed at different locations for each layer of geogrid. The results also indicated that the largest loads were not at the connection between the geogrids and the blocks. The largest tensile load recorded in the second shaking was typically less than 5 kN/m or less than 14% of the ultimate load of the reinforcement. During the introduction of a vertical acceleration in Test 3, an increase in loading at the face was recorded, but the recorded values were always less than the projected values from the hand calculations. This supports the position that the anticipated loads at the face of the wall are substantially less than the calculated maximum tensile loads on the reinforcement. Contrary to calculated loading for geogrids during seismic events at the top of the reinforced mass, loads did not increase during the horizontal and vertical excitations.

Accelerations:

The accelerations in the wall indicated that the amplification was small, less than 1.5. The blocks and backfill were exhibiting similar results in amplification. In Test 3, with a longer top geogrid layer; the phase of amplification was changed such that its magnitude became smaller.

The values of accelerations obtained at the base of shaking table are summarized in the Table 2. The amplification factor is given for the ratio of maximum acceleration in the backfill to the base acceleration. The maximum acceleration is typically recorded at the top of the wall.

Table 2. Acceleration Measured at Shaking Table and Acceleration Amplification

	Test 1	Test 2	Test 3	Test 3 (vertical)
First Shaking	389.9	397.5	406.6	229.9
Second Shaking	858.2	854.8	815.5	395.0
Amplification	1.34	1.16	1.33	--
Unit: gal (1 gal=981cm/s ²)				

Testing Summary

Test Structures and Objectives for each Round of Testing

Structure One:

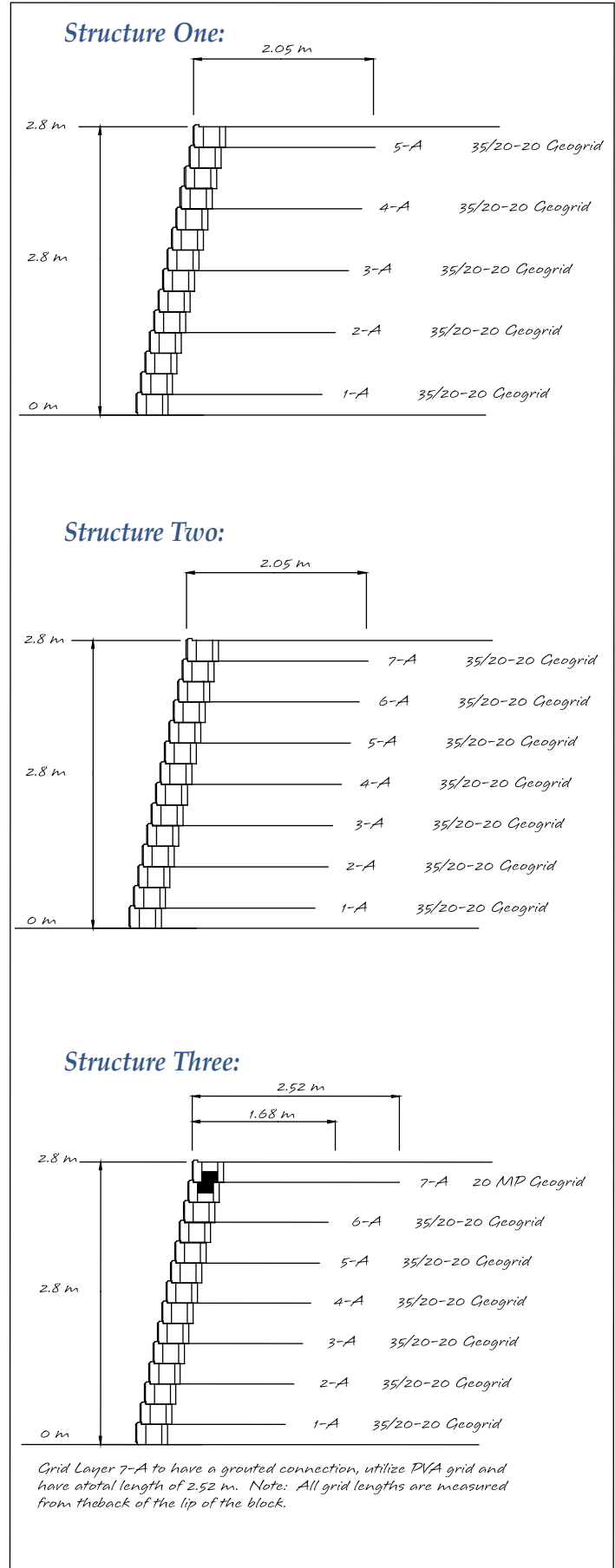
The first round of testing was conducted on a typical configuration of a reinforced soil mass. The base block was placed on 200 mm of sand. The first layer of grid was placed on the first course of block and every 600 mm as the wall was constructed. The lengths of the reinforcement were set at 0.73 times the total height of the wall (2.05 m). Sand was used for reinforced and retained soil zones. Sand was placed to the backside of the block facing and the cores of the blocks were filled with a well-graded gravel.

Structure Two:

The second structure was configured to minimize the settlement that was experienced during the seismic excitation on the first structure. The only change implemented in the second structure was to change the spacing between layers of geogrid. The second structure was constructed with geogrid every 400 mm. By decreasing the spacing there was an expectation that the structure would behave as a more coherent mass and the amount of settlement would be reduced.

Structure Three:

The third structure took into account what had been observed in the testing of the first two structures. The length of the geogrid was shortened to an overall length of 0.6 times the total height of the wall (1.68 m). The top layer of grid was lengthened and grouted into the top two rows of blocks. The top layer of geogrid was changed to a Fortrac 20 MP to eliminate potential damage to the grouted section based on elevated PH of the grouted connection. Additionally the top layer was lengthened to 0.9 times the total height of the wall (2.52 m). The main geogrid lengths were decreased from the previous two structures based on the exceptional performance during the first two rounds of testing. The top geogrid layer was lengthened to transition between the reinforced soil mass and the retained soil mass. The top layer was grouted to the Allan Block units to illustrate how an additional permanent connection element at the top of the wall, could be incorporated into the design.



Testing Results

Summary of Test on the Individual Structures

Structure One:

Each structure was subjected to two independent excitations. The first excitation on Structure One was a horizontal excitation of 0.4g. The observed state of the structure was identical to the as built condition. Residual displacement of the face of the wall measured less than 8mm. Settlement of the reinforced mass measured less than 1mm. Recorded forces in the geogrid layers were at as built levels.

One hour after the original excitation the structure was exposed to a horizontal excitation of 0.8g. The observed state of the structure showed little change from the as built condition. Horizontal displacement was less than 70mm, settlement was largest at the back of the block and was recorded to be less than 90mm. Increase in the load on the grid was minimal and there was no evidence of an internal failure plane. During the excitation it was observed that the reinforced soil mass and the facing were moving in phase.

Structure Two:

The first excitation on Structure Two was a horizontal excitation of 0.4g. The observed state of the structure was identical to the as built condition. Residual displacement of the face of the wall measured less than 5mm. Settlement of the reinforced mass measured less than 1mm. Recorded forces in the geogrid layers were at as built levels.

One hour after the original excitation the structure was exposed to a horizontal excitation of 0.8g. The observed state of the structure showed little change from the as built condition. Horizontal displacement was less than 60mm, settlement was largest at the back of the reinforced mass and was recorded to be less than 30mm. Increase in the load on the grid was minimal and there was no evidence of an internal failure plane. The reduced spacing between grid layers provided a positive benefit creating a structure that performed as a coherent mass. Significant cracking in the retained soil were observed when compared to the reinforced soil zone.

Structure Three:

The first excitation on Structure Three was a horizontal excitation of 0.4g and a vertical excitation of 0.2g. The observed state of the structure was identical to the as built condition. Residual displacement of the face of the wall measured less than 5mm. Settlement of the reinforced mass measured less than 1mm. Recorded forces in the geogrid layers were at as built levels.

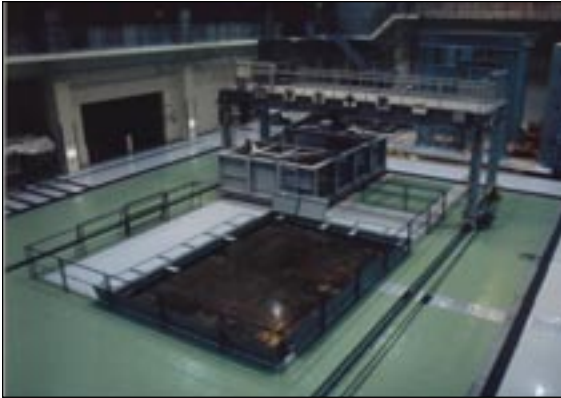
One hour after the original excitation the structure was exposed to a horizontal excitation of 0.8g and a vertical excitation of 0.4g. The observed state of the structure showed no change from the as built condition. Horizontal displacement was less than 50mm, settlement was largest at the back of the top layer of reinforcement and was recorded to be less than 40mm. Increase in the load on the grid was minimal and there was no evidence of an internal failure plane. The increased grid length at the top of the structure pushed the soil cracking back away from the reinforced zone when compared to the first two structures. Even during a combined horizontal and vertical excitation significant loads were not observed at the block to grid connection.

Conclusions:

The results of this study illustrated that the modular block wall system utilizing Allan Block retaining wall units and Huesker geogrid reinforcements performed well under simulated Kobe Earthquake conditions. The deformation and acceleration amplification were negligibly small when subjected to Kobe Earthquake records, showing the reinforced structure absorbs energy from a seismic event. The vertical spacing of 2 blocks (40 cm) and reinforcement lengths of 0.6H with a longer top geogrid layer (0.9H) are adequate to resist a major earthquake provided a good quality backfill is used. Additionally this configuration illustrated that the system performed as a coherent structure with the individual elements in the system remaining in phase during the horizontal and vertical excitations. The hand calculations performed according to the Allan Block Design Methodology provided conservative values based on the observed values on the structures.

It is noted that the reported good measured performance is limited to the tested particular block system and geogrids. The interlocking lip configuration of the Allan Block minimizes differential horizontal movement of the units during earthquake excitation and therefore ensures the integrity of the system. Hence, the results as reported should not be extrapolated to other wall systems, which have different blocks and geogrid reinforcement.

Testing Photos



NRIAE Shaking Table Facility, Tsukuba, Japan



A Layer of White Sand Seam Used to Identify Post-Test Shear Location



Research Team (Left to Right)
Y. Okabe, Y. Mohri, H.I. Ling, T. Kawabata, D. Leshchinsky,
D. Lee, O. Leshchinsky, H. Liu, C. Burke, K. Matsushima



Earth Pressure Transducer Behind the Block and Strain Gages on the Geogrid

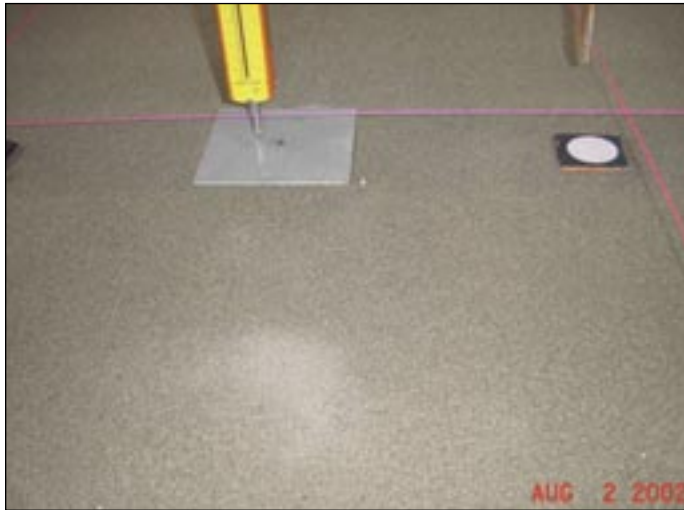


Load Transducers for Measuring Vertical Earth Pressure



LVDT and Markers on the Backfill Surface

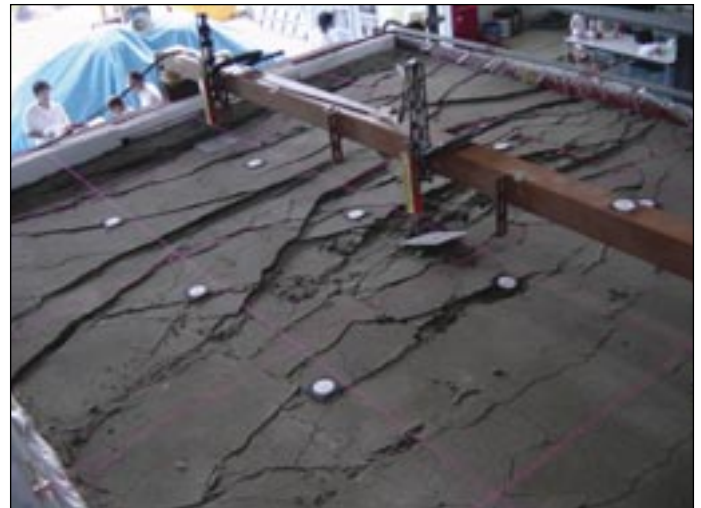
Images of the Seismic Tests using Allan Block and Huesker Geosynthetics



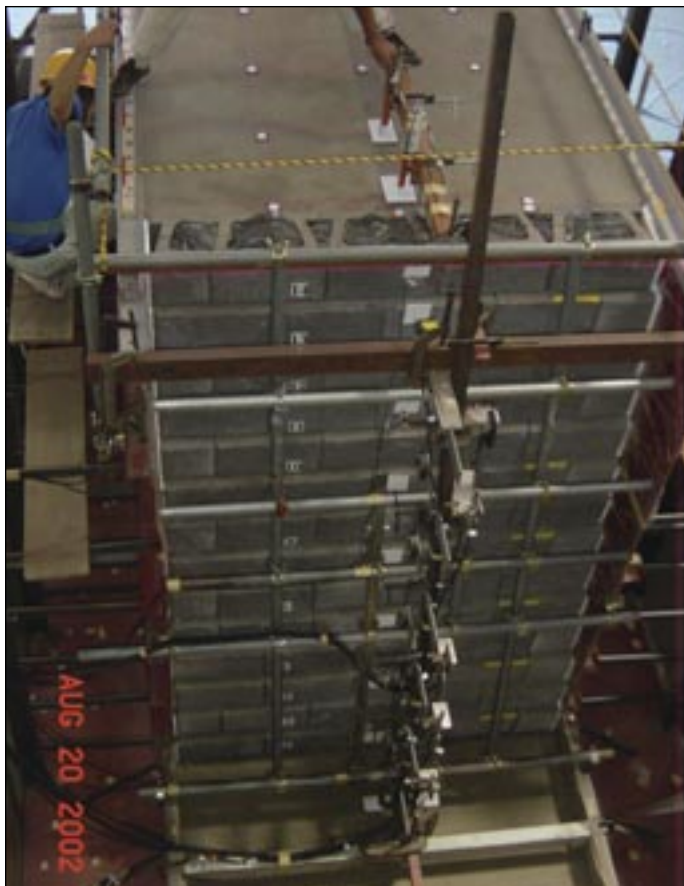
Hair Crack Behind Reinforced Zone after First Shaking Load Application



General Appearance of Test Wall after Second Shaking Load Application



Cracks at the Retained Soil



Completed Structure on Shake Table



Steel Container for Wall Construction

Design Calculations for Static and Seismic Loading using Allan Block Design Methodology

Input Information

Wall Number: Test 3 with 0.8g horizontal acceleration
 Cross Section: Fortrac 35/20-20 Geogrid @ 0.6H and 20MP Geogrid @ 0.9H

Project Name: Seismic Testing
 Columbia University
 Project Number: 1006.02
 Date: 10/09/02
 Prepared By: FMBott, TABott

Allan Block Parameters	Wall Parameters	Footing Dimensions
Block Height: $h = 200 \text{ mm}$	Number of Block Courses: $N = 14$	Footing Width: $L_{\text{width}} = 1.22 \text{ m}$
Block Depth: $t = 296 \text{ mm}$	Total Wall Height: $H = nh = 2.8 \text{ m}$	Footing Depth: $L_{\text{depth}} = 0.3 \text{ m}$
Block Length: $l = 448 \text{ mm}$	Embedment Depth in Courses: $e = 0$	Toe Extension: $L_{\text{toe}} = 0.3 \text{ m}$
Unit Percentage Concrete: $c = 60\%$	Total Embedment Depth: $D = e(h) = 0 \text{ m}$	
Unit Percent Voids: $v = 40\%$	Geogrid Length: $L = 1.68 \text{ m}$	
Block Setback $v = 12^\circ$		

Unit Definition

kN: = 1000 N
 kPa: = 1000 Pa

Back Slope Parameters

Back Slope angle: $i = 0^\circ$
 Back Slope height: $h_i = 15 \text{ m}$

Surcharge Parameters

Surcharge: $q = 0 \text{ kPa}$
 Surcharge Type: $x_q = 3$
 Surcharge Types:
 1 = Retained soil dead load
 2 = Retained soil live load
 3 = Infill soil dead load
 4 = Infill soil live load

Seismic Parameters

Acceleration Coefficient: $A_o = 0.8$
 Allowable Lateral Deflection:
 Internal: $d_i = 50.8 \text{ mm}$
 External: $d_r = 50.8 \text{ mm}$

Point Load Parameters

Point Load: $P = 0 \text{ kN}$
 Contact area boundaries from toe of wall:
 Starting Point: $x_1 = 0 \text{ m}$
 Ending Point: $x_2 = 0 \text{ m}$

Soil Parameters

Infill Soil:

Friction Angle: $\phi_i = 38^\circ$
 Unit Weight: $\gamma_i = 19 \text{ kN/m}^3$

Retained Soil

Friction Angle: $\phi_i = 38^\circ$
 Unit Weight: $\gamma_i = 19 \text{ kN/m}^3$

Foundation Soil

Friction Angle: $\phi_f = 38^\circ$
 Cohesion: $c_f = 0 \text{ kPa}$
 Unit Weight: $\gamma_f = 19 \text{ kN/m}^3$

Geogrid Parameters

Number of geogrid layers: $g = 7$ layers

Geogrid Type A: $A = \text{Fortrac 35/20-20}$

Geogrid Type B: $B = \text{Fortrac 20 MP}$

Long-term Allowable Design Strength

Geogrid Type A: $\text{LTDS}_A = 19.3 \text{ kN/m}$

Geogrid Type B: $\text{LTDS}_B = 13.6 \text{ kN/m}$

Reduction Factor for Long-term Creep

Geogrid Type A: $\text{RFcr}_A = 1.67$

Geogrid Type B: $\text{RFcr}_B = 1.67$

Factor of Safety Geogrid Overstress: $\text{FSos} = 1.5$

Geogrid Interaction Coefficient: $C_i = 0.75$

Geogrid Layout Parameters

Range of Geogrid Layers: $J = g$

Geogrid Coursing	Geogrid Type	Geogrid Length
$\text{grid}_j =$	$\text{type}_j =$	$\text{length}_j =$
13	B	2.5 m
11	A	L
9	A	L
7	A	L
5	A	L
3	A	L
1	A	L

Connection Strength Parameters

Peak Connection Capacity, in the form of linear equation, $y = Mx + B$

Where $y = \text{Connection Strength}$

and $x = \text{Normal Load}$

Geogrid Type A

Segment #1: y intercept: $B_{1a} = 19.16 \text{ kN/m}$ Slope $M_{1a} = 0.14$

Segment #2: y intercept: $B_{2a} = 19.16 \text{ kN/m}$ Slope $M_{2a} = 0.14$

Intersecting Normal Load

$$N_{inta} = \frac{B_{2a} - B_{1a}}{M_{1a} - M_{2a}} \quad N_{inta} = 0 \text{ kN/m}$$

Geogrid Type B

Segment #1: y intercept: $B_{1b} = 10.59 \text{ kN/m}$ Slope $M_{1b} = 0.0524$

Segment #2: y intercept: $B_{2b} = 10.59 \text{ kN/m}$ Slope $M_{2b} = 0.0524$

Intersecting Normal Load

$$N_{intb} = \frac{B_{2b} - B_{1b}}{M_{1b} - M_{2b}} \quad N_{intb} = 0 \text{ kN/m}$$

Broken Back Slope Determination

Broken Back Slope Calculations, i' , only if the horizontal length of the slope is less than twice the wall height.

Determine the true back slope angle:

$$i' = \text{atan} \left(\frac{h_i}{2(H)} \right) \quad i' = 69.528^\circ \quad i = \text{if} (i' \geq i, i, i') \quad \text{Therefore: } i = 0^\circ$$

Calculation of Static and Dynamic Earth Pressure Coefficients

Weighted Friction Angle: $\phi_{wi} = 0.67(\phi_i) = 25.333^\circ$ $\phi_{wr} = 0.67(\phi_r) = 25.333^\circ$

Wall Batter: $\beta = 90^\circ - \omega$ $\beta = 78^\circ$

Setback per Block: $s = 0.0315m + \left(\tan(\omega) \frac{h}{2}\right)$ $s = 0.053m$

Effective Wall Height: $H_e = H + [L - (t - s)] \tan(i)$ $H_e = 2.8m$

Static

Active Earth Pressure Coefficient:

Infill Soil

$$K_{ai} = \left[\frac{\csc(\beta) \sin(\beta - \phi_i)}{\sqrt{\frac{\sin(\beta + \phi_{wi})}{\sin(\beta - i)} + \frac{\sin(\phi_i + \phi_{wi}) \sin(\phi_i - i)}{\sin(\beta - i)}}} \right]^2$$

$K_{ai} = 0.143$

Retained Soil

$$K_{ar} = \left[\frac{\csc(\beta) \sin(\beta - \phi_r)}{\sqrt{\frac{\sin(\beta + \phi_{wr})}{\sin(\beta - i)} + \frac{\sin(\phi_r + \phi_{wr}) \sin(\phi_r - i)}{\sin(\beta - i)}}} \right]^2$$

$K_{ar} = 0.143$

Dymanic

Seismic Coefficients:

$K_v = 0$

Internal Stability

$K_{hi1} = (1.45 - A_o)A_o$ For: $d_i = 0 \text{ mm}$

$K_{hi2} = 0.67(A_o) \left(\frac{(A_o)(25\text{mm})}{d_i} \right)^{0.25}$ For: $d_i > = 25\text{mm}$

$K_{hi} = \text{if}(d_i = 0_{\text{mm}}, K_{hi1}, K_{hi2})$ $K_{hi} = 0.425$

$\theta_i = \text{atan} \left(\frac{K_{hi}}{1 + K_v} \right)$ $\theta_i = 23.005^\circ$

External Stability

$K_{hr1} = A_o$ For: $d_r = 0 \text{ mm}$

$K_{hr2} = 0.67(A_o) \left(\frac{(A_o)(25\text{mm})}{d_r} \right)^{0.25}$ For: $d_r > = 25\text{mm}$

$K_{hr} = \text{if}(d_r = 0_{\text{mm}}, K_{hr1}, K_{hr2})$ $K_{hr} = 0.425$

$\theta_r = \text{atan} \left(\frac{K_{hr}}{1 + K_v} \right)$ $\theta_r = 23.005^\circ$

Dymanic Earth Pressure Coefficient

Infill Soil

$$K_{aei} = \left(\frac{\cos(\phi_i + \omega - \theta_i)^2}{\cos(\theta_i) \cos(\omega)^2 \cos(\phi_{wi} - \omega + \theta_i)} \right) \left(\frac{1}{1 + \sqrt{\frac{\sin(\phi_i + \phi_{wi}) \sin(\phi_i - i - \theta_i)}{\cos(\phi_{wi} - \omega + \theta_i) \cos(\omega + i)}}} \right)^2$$

$K_{aei} = \text{if}(A_o = 0, 0, K_{aei})$ $K_{aei} = 0.471$

Retained Soil

$$K_{aer} = \left(\frac{\cos(\phi_r + \omega - \theta_r)^2}{\cos(\theta_r) \cos(\omega)^2 \cos(\phi_{wr} - \omega + \theta_r)} \right) \left(\frac{1}{1 + \sqrt{\frac{\sin(\phi_r + \phi_{wr}) \sin(\phi_r - i - \theta_r)}{\cos(\phi_{wr} - \omega + \theta_r) \cos(\omega + i)}}} \right)^2$$

$K_{aer} = \text{if}(A_o = 0, 0, K_{aer})$ $K_{aer} = 0.471$

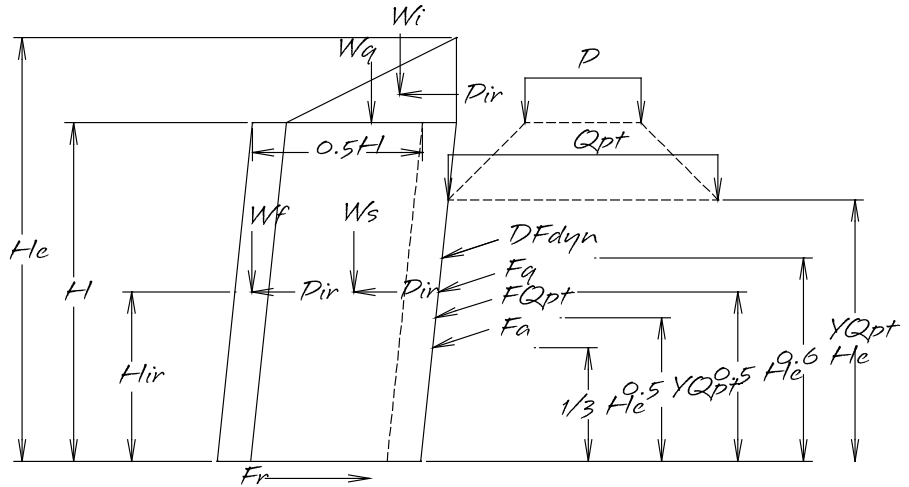
External Stability

External Stability

Free Body Diagram

Where:

- He = Effective Wall Height
- H = Total Wall Height
- Wi = Weight of the Back Slope
- Wq = Infill Surcharge Dead Load
- Wf = Weight of the Allan Block Facing
- Ws = Weight of the Geogrid Reinforced Soil Mass
- Pir = Seismic Inertial Force for each Gravity Force
- Hir = Pir Resultant Vertical Location
- P = Point Load Surcharge
- Qpt = Translated Point Load
- DFdyn = Dynamic Earth Force
- Fq = Surcharge Force
- FQpt = Point Load Force
- YQpt = Translated Point Load Vertical Location
- Fa = Active EarthForce



Concrete Unit Weight: $\gamma_c = 21.207 \text{ kN/m}^3$

Unit Fill Unit Weight: $\gamma_{uf} = 19.636 \text{ kN/m}^3$

Driving Force Calculations

Active Earth Force

$$F_a = 0.5(K_{ar})(\gamma_r)(H_e^2) = 10.667 \text{ kN/m}$$

$$F_{ah} = F_a(\cos(\phi_{WR})) = 9.642 \text{ kN/m}$$

$$F_{av} = F_a(\sin(\phi_{WR})) = 4.564 \text{ kN/m}$$

Dymanic Earth Force

$$F_{ae} = 0.5(1 + K_v)(K_{ae})(\gamma_r)(H_e^2) = 35.07 \text{ kN/m}$$

$$DF_{dyn} = \text{if } (A_o = 0, 0 \text{ kN/m}, DF_{dyn}) = 24.402 \text{ kN/m}$$

$$DF_{dynh} = DF_{dyn}(\cos(\phi_{WR})) = 22.06 \text{ kN/m}$$

$$DF_{dynv} = DF_{dyn}(\sin(\phi_{WR})) = 10.44 \text{ kN/m}$$

$$DF_{dynv} = F_{ae} - F_a = 24.4 \text{ kN/m}$$

Surcharge Force

$$F_q = (q)(K_{ar})(H_e) = 0 \text{ kN/m}$$

$$F_{qh} = (F_q)(\cos(\phi_{WR})) = 0 \text{ kN/m}$$

$$F_{qv} = \text{if } [x_q = 1, F_q(\sin(\phi_{WR})), \text{if } (x_q = 3, F_q(\sin(\phi_{WR})), 0 \text{ kN/m})] = 0 \text{ kN/m}$$

Point Load Surcharge

Elevation of Surcharge above top of wall:

$$Q_h = [x_1 - (t + H(\tan(\omega)))]\tan(i) = 0 \text{ m}$$

Location of the end of grid at the top of the wall plus the influence zone buffer of H/4:

$$End_g = L + s + H(\tan(\omega)) + H/4 = 3.028 \text{ m}$$

Moment Arms:

$$F_a \text{ Arm}_h = 0.33(H_e) = 0.933 \text{ m}$$

$$F_a \text{ Arm}_v = L + s + .33(H_e)(\tan(\omega)) = 1.931 \text{ m}$$

Moment Arms:

$$DF_{dyn} \text{ Arm}_h = 0.6(H_e) = 1.68 \text{ m}$$

$$DF_{dyn} \text{ Arm}_v = L + s + (0.6)(H_e)(\tan(\omega)) = 2.09 \text{ m}$$

Moment Arms:

$$F_q \text{ Arm}_h = (0.5)(H_e) = 1.4 \text{ m}$$

$$F_q \text{ Arm}_v = L + s + (0.5)(H_e)(\tan(\omega)) = 2.03 \text{ m}$$

Minimum application distance for zero influence:

$$\text{Minx1} = L + s + H/4 + \frac{H}{\tan(45^\circ - \phi_r/2)} + \left[\frac{\left(\frac{H}{\tan(45^\circ - \phi_r/2)} + H/4 + L + s - t - H(\tan(\omega)) \right) (\tan(i)) (\sin(90^\circ + i))}{\sin(45^\circ - \phi_r/2 - i)} \right] \cos(45^\circ - \phi_r/2)$$

$$\text{Minx1} = 8.174 \text{ m}$$

Location of the translated point load surcharge:

$$Y_{Qpt} = \left([H + (x1 - (t + H(\tan(\omega)))) \tan(i)] - (x1 - L - s - \frac{H}{4}) (\tan(45^\circ - \phi_r/2)) \right) \left[1 + \sin(45^\circ - \phi_r/2) \left(\frac{\sin(90^\circ + \omega) \tan(\omega)}{\sin(45^\circ + \phi_r/2 - (\omega))} \right) \right]$$

$$Y_{Qpt} = \text{if}(x1 > \text{Endg}, Y_{Qpt}, H_e)$$

$$Y_{Qpt} = 2.8 \text{ m}$$

Location of the end of the grid at the Y_{Qpt} elevation plus the influence zone buffer of $H/4$.

$$\text{Endg}Y_{Qpt} = L + s + Y_{Qpt}(\tan(\omega)) + H/4 = 3.028 \text{ m}$$

The point load will be distributed over its contact area, Q_p and translated through the soil if it acts behind the reinforced mass, Q_{pt} .

$$Q_{pi} = \left(\frac{P}{(x2 - x1)} \right) = 0 \text{ kPa}$$

$$Q_{pti} = \left(\frac{P}{[x1 - \text{Endg}Y_{Qpt}(2) + (x2 - x1)]} \right) = 0 \text{ kPa}$$

Point Load Surcharge Influence

If the point load contact is only with the reinforced mass it will add stability to the wall structure, therefore the loads are only considered in the internal stability calculations.

$$Q_p = \text{if}(x2 \geq L + s + H(\tan(\omega)) - 0.6 \text{ m}, Q_{pi}, 0 \text{ kPa})$$

If the point load contact is beyond the reinforced mass and its influence zone buffer, it will only affect the external stability. If it overlaps both the influence zone and retained soil it will effect both internal and external stability.

$$Q_{pt} = \text{if}(x1 \geq \text{Endg}, Q_{pti}, Q_p)$$

If the point load contact is beyond the reinforced mass plus its influence zone buffer it will have no effect on the wall,

$$Q_{pt} = 0.$$

$$Q_{pt} = \text{if}(x1 > \text{Minx1}, 0 \text{ kPa}, Q_{pt}) = 0 \text{ kPa}$$

Note: Q_{pt} is the translated distributed point load surcharge used to determine the point load force that will be influencing the external stability of the retaining wall structure. Q_{pt} is a function of the location of the contact area with respect to the geogrid reinforcement. Q_p will be used to calculate the point load surcharge if it acts directly on top of the reinforced soil. No translation calculations are necessary for Q_p because its applications area is on top of the reinforced mass and its influence zone buffer.

Point Load Surcharge

$$FQ_{pt} = (Q_{pt})(K_{ar})(Y_{qpt}) = 0 \text{ kN/m}$$

$$FQ_{pth} = FQ_{pt}(\cos(\phi_{WR})) = 0 \text{ kN/m}$$

Point Load Surcharge Weight

$$WQ_{pt1} = Q_{pi}(x_2 - 1)$$

$$WQ_{pt2} = Q_{pi}(L + s + H(\tan(\omega)) - x_1)$$

$$WQ_{pt} = \text{if } (x_2 \leq L + s + H(\tan(\omega)) - 0.6 \text{ m}, WQ_{pt1}, WQ_{pt2})$$

$$WQ_{pt} = \text{if } (x_1 \leq L + s + H(\tan(\omega)), 0 \text{ kN/m}, WQ_{pt})$$

$$WQ_{pt} = 0 \text{ kN/m}$$

Moment Arms:

$$FQ_{ptArmh} = Y_{qpt}/2 = 1.4 \text{ m}$$

Moment Arms:

$$WQ_{ptArm1} = x_1 + \frac{(x_2 - x_1)}{2}$$

$$WQ_{ptArm2} = x_1 + \left(\frac{(\text{Endg} - H/4 - x_1)}{2} \right)$$

$$WQ_{ptArm} = \text{if } (x_2 \leq L + s + H(\tan(\omega)) - 0.6 \text{ m}, WQ_{ptArm1}, WQ_{ptArm2})$$

$$WQ_{ptArm} = 0 \text{ m}$$

Resisting Force Calculations**Weight of the Back Slope**

$$W_i = 0.5 \gamma y (H_e - H) [L - (t - s)] = 0 \text{ kN/m}$$

Weight of the Dead Load Surcharge

$$W_q = \text{if } (x_q = 3, [L - (t - s)] q, 0 \text{ kN/m})$$

Weight of the Facing

$$W_f = H(t)[(c)(\gamma_c) + (v)(\gamma_{uf})] = 17.056 \text{ kN/m}$$

Weight of the Reinforced Soil Mass

$$W_s = H[L - (t - s)] \gamma_i = 76.435 \text{ kN/m}$$

Total Weight

$$W_t = W_f + W_s = 93.491 \text{ kN/m}$$

Sliding Resistance

$$F_{rstatic} = (F_{av} + F_{qv} + W_i + W_q + W_f + W_s) \tan(\phi_i)$$

$$= 76.609 \text{ kN/m}$$

Moment Arms:

$$W_iArm = 0.67 [L - (t - s)] + H(\tan(\omega)) + t = 1.849 \text{ m}$$

$$W_qArm = 0.5 [L - (t - s)] + H(\tan(\omega)) + t = 1.61 \text{ m}$$

$$W_tArm = 0.5 (L + s) + 0.5 H(\tan(\omega)) = 1.164 \text{ m}$$

$$F_{rseismic} = (F_{av} + DF_{dynv} + F_{qv} + W_i + W_q + W_f + W_s) \tan(\phi_i) = 84.767 \text{ kN/m}$$

Seismic Inertial Force

The weight of each component of the wall structure has a horizontal inertial force acting at its centroid during a seismic event. The three components that have this inertial force are the block facing, the reinforced soil mass and the Back Slope soil. The resultant P_{ir} is the sum of all three. The weight of the reinforced soil mass and the Back Slope soil is based on a reinforcement length of 0.5 H.

Weight of the Block Face

$$W_f = 17.056 \text{ kN/m}$$

Seismic Inertial Force

$$P_{ir} = K_{hr}(W_f + W_s' + W_i') = 33.37 \text{ kN/m}$$

Moment Arm

$$H_{ir} = \frac{K_{hr} (W_f)(H/2) + K_{hr}(W_s)(H/2) + K_{hr}(W_i') [H + 0.33[0.5 H - (t - s)] \tan(i)]}{P_{ir}} = 1.4 \text{ m}$$

Weight of the Reinforced Soil Mass

$$W_s' = [0.5 H - (t - s)] \gamma_i H = 61.539 \text{ kN/m}$$

Weight of the Back Slope

$$W_i' = 0.5 [0.5 H - (t - s)]^2 \gamma_r \tan(i) = 0 \text{ kN/m}$$

External Stability Factors of Safety

Factor of Safety for Sliding

Static Conditions: $FS_{staticsliding} \geq 1.5$

$$FS_{staticsliding} = \frac{Fr_{static}}{F_{ah} + F_{qh} + F_{Qpth}} = 7.95$$

Seismic Conditions: $FS_{seismicsliding} \geq 1.1$

$$FS_{seismicsliding} = \frac{Fr_{seismic}}{F_{ah} + DF_{dynh} + F_{qh} + F_{Qpth} + P_{ir}} = 1.3$$

Factor of Safety for Overturning

Static Conditions: $FS_{staticoverturning} \geq 2.0$

$$FS_{staticoverturning} = \frac{W_t(W_tArm) + W_i(W_iArm) + W_q(W_qArm) + F_{av}(F_{aArm}v) + F_{qv}(F_{qArm}v)}{F_{ah}(F_{aArm}h) + F_{qh}(F_{qArm}h) + F_{Qpth}(F_{QptArm}h)} = 13.07$$

Seismic Conditions: $FS_{seismicoverturning} \geq 1.5$

$$FS_{seismicoverturning} = \frac{W_t(W_tArm) + W_i(W_iArm) + W_q(W_qArm) + F_{av}(F_{aArm}v) + F_{qv}(F_{qArm}v) + DF_{dynv}(DF_{dynArm}v)}{F_{ah}(F_{aArm}h) + DF_{dynh}(DF_{dynArm}h) + F_{qh}(F_{qArm}h) + F_{Qpth}(F_{QptArm}h) + P_{ir}(H_{ir})} = 1.5$$

Bearing Capacity Calculations - Standard Method

Vertical Force Resultant

$$R = W_f + W_s + W_i + W_q + F_{av} + DF_{dynv} + F_{qv} + W_{Qpt} = 108.497 \text{ kN/m}$$

Location of the Resultant Force

$$\text{positive} = W_t(W_tArm) + W_i(W_iArm) + W_q(W_qArm) + W_{Qpt}(W_{QptArm}) + F_{av}(F_{avArm}v) + DF_{dynv}(DF_{dynArm}v) + F_{qv}(F_{qArm}v)$$

$$\text{negative} = F_{ah}(F_{aArm}h) + DF_{dynh}(DF_{dynArm}h) + F_{qh}(F_{qArm}h) + F_{Qpth}(F_{QptArm}h) + P_{ir}(H_{ir})$$

$$\text{positive} = 139.455 \text{ kN}$$

$$\text{negative} = 92.77 \text{ kN}$$

$$x = \frac{\text{positive} - \text{negative}}{R} = 0.43 \text{ m}$$

Determine the eccentricity, E, of the resultant vertical force.

$$E = 0.5(L + s) - x = 0.436 \text{ m}$$

Determine the average bearing pressure acting at the centerline of the wall.

$$\sigma_{avg} = \frac{R}{(L + s)} = 62.615 \text{ kPa}$$

Determine the moment about the centerline of the wall due to the resultant bearing load.

$$M_{cl} = R(E) = 47.314 \text{ kN/m}^2$$

$$\text{section modulus } S = \frac{(1.0 \text{ m})(L + s)^2}{6} = 0.5 \text{ m}^3$$

Difference in bearing pressure due to the eccentric loading.

$$\sigma_{\text{mom}} = \frac{M_{\text{cl}} (1 \text{ m})}{S} = 94.551 \text{ kPa}$$

Therefore:

$$\sigma_{\text{max}} = \sigma_{\text{avg}} + |\sigma_{\text{mom}}| = 157.166 \text{ kPa}$$

$$\sigma_{\text{min}} = \sigma_{\text{avg}} - |\sigma_{\text{mom}}| = 31.936 \text{ kPa}$$

Ultimate Bearing Capacity Calculations

Meyerhoff bearing capacity equation

$$\sigma_{\text{ult}} = 0.5 \cdot \gamma_f \cdot L_{\text{width}} \cdot N_{\gamma} + c_f \cdot N_c + \gamma_f \cdot (L_{\text{depth}} + D) \cdot N_q$$

$$\text{Where: } N_q = (\exp(\pi \tan(\phi_f)))[\tan(45^\circ + \frac{\phi_f}{2})]^2 = 48.933$$

$$N_c = (N_q - 1) \cot(\phi_f) = 61.352$$

$$N_{\gamma} = (N_q - 1) (\tan(1.4)(\phi_f)) = 64.074$$

Therefore:

$$\sigma_{\text{ult}} = 0.5(\gamma_f)(L_{\text{width}})(N_{\gamma}) + c_f(N_c) + \gamma_f(L_{\text{depth}} + D)N_q = 1021.534 \text{ kPa}$$

Factor of Safety

$$FS_{\text{bearing}} = \frac{\sigma_{\text{ult}}}{\sigma_{\text{max}}} \quad FS_{\text{bearing}} = 6.5$$

Internal Stability

Internal Stability

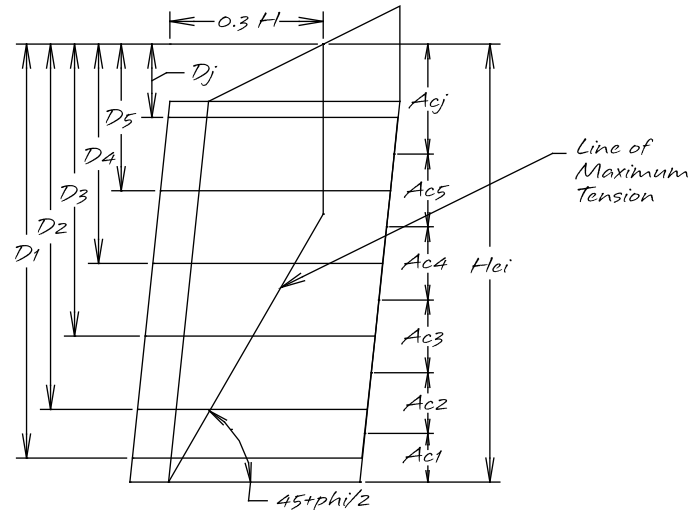
Free Body Diagram

Where:

- D_j = Depth to each Geogrid Layer
- $0.3H$ = Orientation of line of Maximum Tension
- $45+\phi/2$ = Orientation of the line of Maximum Tension
- A_{c_j} = Influence area of each Geogrid Layer
- H_{ei} = Effective Wall Height for Internal Stability

Grid Elevation: $elev_j = grid_j(h)$

$$H_{ei} = H + [0.3 H - (t - s)] \tan(i) = 2.8 \text{ m}$$



Note: For internal stability calculations sample calculations will be shown for grid layer #1. All other grid layers will be shown through tabular calculations at the end of this section.

Determination Of The Force Acting On Each Grid Layer

Static Loads, use the subscript "s".

Influence Area

$$A_{c_j} = \text{if } \left(j = 1, \frac{grid_{j+1}(h) + grid_j(h)}{2} \right),$$

$$\text{if } \left(j = g, H_{ei} - \left(\frac{grid_j(h) + grid_{j-1}(h)}{2} \right), \left(\frac{grid_{j+1}(h) + grid_j(h)}{2} \right) - \left(\frac{grid_j(h) + grid_{j-1}(h)}{2} \right) \right)$$

$$= 0.4 \text{ m}$$

Active Earth Pressure

$$G_j = \text{if } \left(j = g, H_{ei} - \left(\frac{grid_j(h) + grid_{j-1}(h)}{2} \right), H_{ei} - \left(\frac{grid_{j+1}(h) + grid_j(h)}{2} \right) + H_{ei} - \left(\frac{grid_j(h) + grid_{j-1}(h)}{2} \right) \right)$$

$$F_{a_j} = K_{ai} (\cos(\phi_{wi})) (\gamma_i) (A_{c_j}) (0.5) \text{ if } \left(j = 1, H_{ei} + \left(H_{ei} - \left(\frac{grid_{j+1}(h) + grid_j(h)}{2} \right) \right), G_j \right)$$

$$F_{a_j} = 2.558 \text{ kN/m}$$

Surcharge Pressure

$$F_{q_j} = \text{if } (x_q = 3, q(K_{ai})(\cos(\phi_{wi}))(A_{c_j}), \text{ if } x_q = 4, q(K_{ai})(\cos(\phi_{wi}))(A_{c_j}), 0 \text{ Kn/m}) = 0 \text{ kN/m}$$

Point Load Surcharge Pressure

$$F_{Q_{pt_j}} = \text{if } (x_1 > (L + s + H \tan(\omega)) + 0.6 \text{ m}, 0 \text{ kN/m}, Q_{pt}(K_{ai})(\cos(\phi_{wi}))(A_{c_j})) = 0 \text{ kN/m}$$

Seismic (Dynamic) Loads, use the subscript "d".

Dynamic Earth Pressure

$$DF_{dynj} = \left(0.8 - (0.6) \left(\frac{Hei - grid_j(h)}{Hei} \right) \right) K_{aei} (\cos(\phi_{wi})) (\gamma_i) (Hei) (Ac_j) = 2.199 \text{ kN/m}$$

Seismic Inertial Force

$$P_{irj} = K_{hi}(t) \left((c)(\gamma_c) + v(\gamma_{uf}) \right) Ac_j = 1.034 \text{ kN/m}$$

Tensile Force on Each Geogrid

Static

$$F_{isj} = F_{aij} + F_{qij} + F_{Qptij} = 2.558 \text{ kN/m}$$

Seismic

$$F_{idj} = F_{aij} + F_{qij} + F_{Qptij} + DF_{dynj} + P_{irj} = 5.792 \text{ kN/m}$$

Geogrid Tensile Overstress

Geogrid Tensile Strength

$$LTDS_j = \text{if}(\text{type}_j = A, LTDS_A, LTDS_B) = 19.3 \text{ kN/m}$$

$$RF_{crj} = \text{if}(\text{type}_j = A, RF_{cr_A}, RF_{cr_B}) = 1.67$$

Factor of Safety, Static

$$FS_{overstress} = \frac{LTDS_j}{F_{isj}} = 7.545$$

Factor of Safety, Seismic

$$FS_{overstressdj} = \frac{LTDS_j(RF_{crj})}{F_{idj}} = 5.565$$

Geogrid / Block Connection Capacity

Normal Load

$$N_j = (H - grid_j - h)[c(\gamma_c) + v(\gamma_{uf})t] = 15.837 \text{ kN/m}$$

Peak Connection Strength

$$F_{csj} = \text{if}[\text{type}_j = A, \text{if}(N_j < N_{inta}, B1a + M1a(N_j)), \text{if}(N_j < N_{intb}, B1b + M1b(N_j), B2b + M2b(N_j))] = 21.377 \text{ kN/m}$$

Factor of Safety Connection Strength, Static

$$FS_{connsj} = \frac{F_{csj}}{F_{isj}(0.667)} = 12.529$$

Factor of Safety Connection Strength, Seismic

$$FS_{connndj} = \frac{F_{csj}}{F_{idj}(0.667)} = 5.534$$

Geogrid Pullout from the Soil

Equations for each segment of the line of maximum tension:

$$\text{segment \#1: } y_1 = \tan(45^\circ + \phi/2)(x-t) \quad \text{where } x = \text{distance to the line of maximum tension.}$$

$$\text{segment \#2: } x = (H)(0.3 + \tan(\omega))$$

Setting these two equations equal to each other yields the elevation of their intersection point.

$$y_{int} = \tan(45^\circ + \phi_i/2) [H(0.3 + \tan(\omega)) - t] = 2.336 \text{ m}$$

Therefore the length of geogrid embedded beyond the line of maximum tension is the following.

For geogrid elevation < y_{int}

$$Le_{1j} = (\text{length}_j + s) - \left(\left(\frac{\text{grid}_j(h)}{\tan(45^\circ + \phi_i/2)} \right) + t \right) + (\tan(\omega))[(\text{grid}_j)(h)]$$

For geogrid elevation > yint

$$Le_{2j} = (\text{length}_j + s) - H(0.3 + \tan(\omega)) + (\tan(\omega))[(\text{grid}_j)(h)]$$

Geogrid Embedment Length

$$Le_j = \text{if}(\text{grid}_j(h) < y_{\text{int}}, Le_{1j}, Le_{2j}) = 1.382 \text{ m}$$

Surcharge Geogrid Length

$$Lq_j = \text{if}(x_q = 3, Le_j, Om) = 1.382 \text{ m}$$

Pullout Capacity

$$Fp_j = 2(C_i)(\tan(\phi_i)) [(H_{ei} - \text{grid}_j(h)) \gamma_i(Le_j) + q(Lq_j)] = 79.992 \text{ kN/m}$$

Factor of Safety Geogrid Pullout, Static

$$FS_{\text{pullouts}_j} = \frac{Fp_j}{Fis_j} = 31.272$$

Factor of Safety Geogrid Pullout, Dynamic

$$FS_{\text{pulloutd}_j} = \frac{Fp_j}{Fid_j} = 13.811$$

Geogrid Efficiency

Static Conditions

$$\text{effecs}_j = \frac{Fis_j}{LTDS_j(0.67)} (100) = \text{effecs}_1 = 19.881$$

Seismic Conditions

$$\text{effecsd}_j = \frac{Fid_j}{LTDS_j(RF_{crj} / 1.1)} (100) = \text{effecd}_1 = 19.767$$

Localized Stability, Top of the Wall Stability

Local Wall Parameters

$$\text{Unreinforced Height: } Ht = H - \text{grid}_g(h) = 0.2 \text{ m}$$

$$\text{Local Weight of Facing: } Wft = Ht(t)[(c)(\gamma_c) + v(\gamma_{uf})] = 1.218 \text{ kN/m}$$

$$\text{Local Slide Resistance: } Frt = 11.7 \text{ kN/m} + Wft (\tan)(56^\circ) = 13.506 \text{ kN/m}$$

Note: This equation is based on the Allan Block shear strength. The equation was developed through empirical test data and is a function of the normal load acting at that point.

Soil and Surcharge Forces

$$\text{Active Force: } Fat = 0.5(K_{ai})(\gamma_i)(Ht)^2 = 0.054 \text{ kN/m}$$

$$\text{Dynamic Force: } Faet = 0.5(1 + K_v)(K_{aei})(\gamma_i)(Ht)^2 = 0.179 \text{ kN/m}$$

$$DFdynt = Faet - Fat = 0.125 \text{ kN/m}$$

$$DFdynt = \text{if}(A_o - 0, 0 \text{ kN/m}, DFdynt) = 0.125 \text{ kN/m}$$

Seismic Inertial Force

$$Pirt = K_{hi}(Wft) = 0.517 \text{ kN/m}$$

Surcharge Force

$$Fqt = \text{if}(x_q = 3, q(K_{ai})(Ht), \text{if}(x_q = 4, q(K_{ai})(Ht), 0 \text{ kN/m})) = 0 \text{ kN/m}$$

Point Load Surcharge

$$FQptt = \left(\text{if} [x_1 - (H(\tan(\omega)) + t)] < \frac{Ht}{\tan(45^\circ + \phi_i/2)}, Q_{pt}, K_{ai}, Ht, 0 \text{ kN/m} \right) = 11.7 \text{ kN/m}$$

Factor of Safety Local Sliding, Static

$$FS_{slidingst} = \frac{F_{rt}}{(F_{at} + F_{qt} + F_{Qptt}) \cos(\phi_{wi})} = 274.559$$

Factor of Safety Local Sliding, Seismic

$$FS_{slidingdt} = \frac{F_{rt}}{(F_{at} + DF_{dynt} + F_{qt} + F_{Qptt} + P_{irt}) \cos(\phi_{wi})} = 21.465$$

Factor of Safety Local Overturning - Static

$$FS_{overturningst} = \frac{W_{ft} \left(\frac{Ht}{2} \tan(\omega) + \frac{t}{2} \right) + F_{at} (\sin(\phi_{wi})) \left(\frac{Ht}{3} (\tan(\omega)) + t \right) + F_{qt} (\sin(\phi_{wi})) \left(\frac{Ht}{2} \tan(\omega) + t \right)}{F_{at} (\cos(\phi_{wi})) \left(\frac{Ht}{3} \right) + F_{qt} (\cos(\phi_{wi})) \left(\frac{Ht}{2} \right) + F_{Qptt} (\cos(\phi_{wi})) \left(\frac{Ht}{2} \right)}$$

$$FS_{overturningst} = 65.077$$

Factor of Safety Local Overturning - Seismic

$$FS_{overturningst} =$$

$$\frac{W_{ft} \left(\frac{Ht}{2} (\tan(\omega)) + \frac{t}{2} \right) + F_{at} (\sin(\phi_{wi})) \left(\frac{Ht}{3} (\tan(\omega)) + t \right) + F_{qt} (\sin(\phi_{wi})) \left(\frac{Ht}{2} (\tan(\omega)) + t \right) + DF_{dynt} (\sin(\phi_{wi})) (0.6 (Ht) + t)}{F_{at} (\cos(\phi_{wi})) \left(\frac{Ht}{3} \right) + DF_{dynst} (\cos(\phi_{wi})) [(0.6)(Ht)] + F_{qt} (\cos(\phi_{wi})) \left(\frac{Ht}{2} \right) + F_{Qptt} (\cos(\phi_{wi})) \left(\frac{Ht}{2} \right) + P_{irt} \left(\frac{Ht}{2} \right)}$$

$$FS_{overturningdt} = 3.439$$

For the mathcad file, please contact the AB Engineering Department.

Summary of Calculations

Summary of Results

Design Parameters:

Wall Height	$H = 2.8$ m
Block Setback	$\omega = 12^\circ$
Back Slope Angle	$i = 0^\circ$
Back Slope Height	$h_i = 0$ m
Surcharge Load	$q = 0$ kPa
Point Load Surcharge	$P = 0$ kN
Point Load Location	$x_1 = 0$ m $x_2 = 0$ m
Seismic Coefficient	$A_o = 0.8$
Allowable Deflection	
Internal	$d_i = 50.8$ mm
External	$d_r = 50.8$

Soil Parameters:

Infill Soil	$\phi_i = 38^\circ$ $\gamma_i = 19$ kN/m ³
Retained Soil	$\phi_r = 38^\circ$ $\gamma_r = 19$ kN/m ³
Foundation Soil	$\phi_f = 38^\circ$ $\gamma_f = 19$ kN/m ³ $c_f = 0$ kPa

Geogrid Parameters:

Geogrid Type A	A = Fortrac 35/20-20
Geogrid Type B	B = Fortrac 20 Mp
Number of Layers	$g = 7$ layers
Geogrid Length	$L = 1.68$ m

External Stability

Static Conditions

Factor of Safety for Sliding
 $FS_{staticsliding} = 7.95$

Factor of Safety for Overturning
 $FS_{staticoverturning} = 13.07$

Base Footing Dimensions

Width of Footing $L_{width} = 1.22$ m
Width of Reinforcement $L_{grid} = 1.22$ m
Toe Extension $L_{toe} = 0.3$ m
Depth of Footing $L_{depth} = 0.3$ m

Seismic Conditions

Factor of Safety for Sliding
 $FS_{seismicsliding} = 1.3$

Factor of Safety for Overturning
 $FS_{seismicoverturning} = 1.5$

Bearing Capacity

Ultimate Bearing $\sigma_{ult} = 1022$ kPa
Bearing Pressure $\sigma_{max} = 157$ kPa
Factor of Safety $FS_{bearing} = 6.5$

When reinforcement is present it shall always be placed 150 mm from the bottom of the footing.

Note: The minimum footing dimensions are 150 mm deep by 600 mm wide. If the values specifying the footing dimensions are not greater than 150 mm deep by 600 mm wide, the minimum size should be used. When geogrid reinforcement is present the minimum footing depth shall be 300 mm to provide 150 mm of cover above and below the geogrid.

Internal Stability Local Top of Wall Stability

Static Conditions

Factor of Safety for Sliding
 $FS_{slidest} = 274.56$

Factor of Safety for Overturning
 $FS_{overturningst} = 65.08$

Seismic Conditions

Factor of Safety for Sliding
 $FS_{slidingdt} = 21.46$

Factor of Safety for Overturning
 $FS_{overturningdt} = 3.44$

Internal Stability

Static Conditions

Geogrid Length L = 1.68 m

Top Layer L = 2.52 m

Geogrid Number	Geogrid Elevation m	Allowable Load kN/m	Tensile Force kN/m	Factor of Safety Overstress	Factor of Safety Pullout, Block	Factor of Safety Pullout, Soil	Geogrid Efficiency, %
j =	elev _j =	$\frac{LTDS_j}{1.5} =$	Fis _j =	FSoverstress _j =	FScnns _j =	FSpullouts _j =	effecs _j =
7	2.6	9.067	0.197	69.117	81.176	37.802	2.17
6	2.2	12.867	0.59	32.695	49.962	18.816	4.588
5	1.8	12.867	0.984	19.617	30.497	21.307	7.646
4	1.4	12.867	1.377	14.012	22.155	23.798	10.705
3	1.0	12.867	1.771	10.898	17.52	26.289	13.764
2	0.6	12.867	2.164	8.917	14.571	28.78	16.822
1	0.2	12.867	2.558	7.545	12.529	31.272	19.881

Internal Stability

Seismic Conditions

Geogrid Length L = 1.68 m

Top Layer L = 2.52 m

Geogrid Number	Geogrid Elevation m	Allowable Load kN/m	Tensile Force kN/m	Factor of Safety Overstress	Factor of Safety Pullout, Block	Factor of Safety Pullout, Soil	Geogrid Efficiency, %
j =	elev _j =	$LTDS_j \left(\frac{RF_{ct}}{1.1} \right) =$	Fid _j =	FSoverstress _{dj} =	FScnnd _j =	FSpullout _{dj} =	effecd _j =
7	2.6	20.647	8.088	2.808	1.975	0.92	39.173
6	2.2	29.301	7.706	4.183	3.827	1.441	26.298
5	1.8	29.301	7.323	4.401	4.097	2.863	24.992
4	1.4	29.301	6.94	4.644	4.397	4.723	23.685
3	1.0	29.301	6.557	4.915	4.732	7.1	22.379
2	0.6	29.301	6.175	5.22	5.108	10.089	21.073
1	0.2	29.301	5.792	5.565	5.534	13.811	19.767

Allan Block Corporation and Huesker Synthetics

Allan Block Corporation

The Allan Block Company was started in 1986 by Robert Allan (Bob) Gravier. Over the last decade, Allan Block has become a prominent retaining wall company worldwide. The company began with the introduction of their patented segmental retaining wall product - the Original Allan Block. The introduction of this stackable retaining wall system was an overwhelming industry success.

The patented system offers the easiest, most durable and most cost effective product on the market. This coupled with the flexibility of design, wide assortment of sizes, styles and colors makes the Allan Block product line the preferred product for retaining wall construction around the world. Allan Block's commitment and investment into research and testing gives our consumers confidence in a quality product.

The Allan Block network is a team of professionals dedicated to producing, distributing, designing and constructing the Allan Block products. This network is continually expanding, as enthusiasm and support for our company rapidly grows. We have built strong relationships with over 40 manufacturers in North America and over 30 overseas, who help us transfer our products and technology across the globe.



Allan Block reinforced with Huesker geogrid.

Huesker Geosynthetics

The company was founded as a weaving mill in 1861. HUESKER has been producing geotextiles since the 1950's. Today, HUESKER provides a wide, application-oriented range of synthetic wovens, geogrids, composites, clay liners as well as nonwovens and drainage composites.

Much of the manufacturing equipment has been internally developed, being optimized to suit specific product lines. HUESKER uses synthetic filament yarns and fibers of various high quality polymers in the manufacturing of technical textile products.

In addition to its standard products, HUESKER works closely with customers, engineering consultants, research bodies and test institutes to develop individual products and solutions for the most varied of construction-industry applications.





allanblock.com